Synthesis of heavy nuclei using damped collisions: A test

W. Loveland, A. M. Vinodkumar, D. Peterson, and J. P. Greene

The Synthesis of Heavy Nuclei Using Damped Collisions–A Test

W. Loveland, A.M. Vinodkumar

Department of Chemistry, Oregon State University, Corvallis, OR 97331, USA

D. Peterson and J.P. Greene

Physics Division, Argonne National Laboratory, Argonne, IL 60439, USA

(Dated: March 21, 2011)

Abstract

We have measured the angular distributions and production cross sections for the products of the reaction of 859 MeV ($E_{c.m.}$ = 461.9 MeV) ^{160}Gd with ^{186}W. We detected fragments that stopped in the 5.775 mg/cm^2 target as well as fragments emerging at 9-17°, 17-90° and 90-180°. We also made a chemical separation of the Pb isotopes formed in this reaction. An unusually large yield of trans-target reaction products near Z=79 was observed. We compare these observations with the recent predictions of Zagrebaev and Greiner for this reaction.

PACS numbers: 25.70.Jj,25.85.-w,25.60.Pj,25.70.-z

I. INTRODUCTION

In Figure 1, we show the current situation with regard to the synthesis of superheavy nuclei using cold fusion and hot fusion reactions. (Cold fusion reactions involve the use of ^{208}Pb or ^{209}Bi target nuclei leading to the formation of evaporation residues (ERs) with an excitation energy (E*) of $\sim$ 13 MeV which results in a high survival against fission. Hot fusion reactions involve the use of actinide target nuclei, lighter projectiles and lead to the production of highly excited ERs (E*=30-60 MeV) with lower survival against fission. For review articles summarizing recent progress in this field, see [1–5]) For cold fusion syntheses, the production cross sections decrease with increasing atomic number of the completely fused system, Z_{CN}, until one reaches element 113 where the measured fusion cross section is 32 fb, a production rate of about 1 atom/year. Even with the modest expected increase in production cross section for element 114, further use of this path to the superheavy nuclei will require significant technical advances.

For syntheses involving hot fusion reactions, the cross sections decrease significantly from Z=102 to Z=110 and then decrease more slowly until Z=118 where the production cross section is 0.5 pb. Attempts to synthesize element 120 by the ^{64}Ni + ^{238}U reaction and the ^{58}Fe + ^{244}Pu reaction have resulted in upper limit cross sections of about 0.1 pb and 0.4 pb, respectively. [6, 7]. In view of this situation, there has been a revival of interest in the use of damped collisions of massive nuclei at near barrier energies to synthesize superheavy nuclei, particularly those nuclei with large neutron excess, approaching the N=184 shell. In the 1980s [8] there were attempts to use the ^{238}U + ^{238}U and the ^{238}U + ^{248}Cm reactions at above barrier energies to produce trans-target nuclides. While there was evidence for the formation of neutron-rich isotopes of Fm and Md at the 0.1 μb level, no higher actinides were found. The fundamental problem was that the nuclei that were produced far above the target nucleus were the result of events with high total kinetic energy loss, i.e., high excitation energies and resulting poor survival probabilities. Very recently, Zagrebaev and Greiner [9, 10, 12–17] using a new model [11] for these collisions, have examined the older experiments and some proposed new experiments (^{232}Th +^{250}Cf, ^{238}U+^{238}U, and ^{238}U +^{248}Cm). With their new model which emphasizes the role of shell effects in damped collisions, they are able to correctly describe the previously measured fragment angular, energy and charge distributions from the ^{136}Xe + ^{209}Bi reaction and the isotopic yields of Cf , Es, Fm and Md

from the ^{238}U + ^{248}Cm reaction. They predict that by a careful choice of beam energies and projectile-target combinations, one might be able to produce n-rich isotopes of element 112 in the ^{248}Cm +^{250}Cf reaction. They suggest the detection of ^{267,268}Db and ^{272,271}Bh (at the pb level) in the Th + Cf or U + Cm reactions to verify these predictions. Such experiments are very difficult because of the low cross sections, the lower intensities of these massive projectile beams and the problems of detecting the reaction products in an ocean of elastically scattered particles, etc.

However, in 2007, Zagrebaev and Greiner [18] outlined a simpler test of their theoretical predictions. They applied the same model used to study the U + Cm, Th + Cf and U + U collisions to the ^{160}Gd + ^{186}W reaction. The predicted mass yield distributions and the yields of the Pb transfer products (ΔZ = + 8) are shown in Figure 2. The predicted mass yields range from 1-100 mb while the Pb isotopic yields range from 1-5 mb. Other models for producing trans-target nuclides in massive damped collisions have been discussed elsewhere[19–21]. Based upon our prior experience of determining fragment mass and isotropic distributions in the reaction of low energy, intermediate energy and relativistic heavy ions with Ta, Au and Pb, [22–55] we concluded that these same quantities could be determined in the reaction of 856 MeV ^{160}Gd with ^{186}W. We also note similar measurements by Asano et al. for the proton induced spallation of W [56].

II.   EXPERIMENTAL METHOD

The experiment took place in the ATSCAT chamber at the ATLAS facility at the Argonne National Laboratory. A beam of 960 MeV ^{160}Gd struck a 5.775 mg/cm^2 foil of ^{186}W (99 percent enriched) mounted at the center of the chamber. The center of target beam energy was 859 MeV ($E_{c.m.}$ = 461.9 MeV). A deep suppressed Faraday cup at the exit of the chamber was used to monitor the beam intensity. The average on-target projectile intensity was 70 enA of ^{160}Gd^{34+}. The foil was irradiated for 19 hours. The target-catcher foil assembly is shown schematically in Figure 4. The experimental geometry used was that of a cylinder lined with catcher foils. The cylinder was 16 cm in length with a diameter of 5 cm. A 1 cm diameter hole allowed the beam to enter the chamber and a 2.54 cm diameter hole allowed the beam to exit the chamber. The top half of the cylinder was lined with 9.7 mg/cm^2 Mylar foil (shown in blue) while the bottom half of the cylinder was covered by 13.5 mg/cm^2 Al foil

(shown in red). These foils should stop all reaction products. After irradiation, the catcher foils were divided into three samples, "backward", "forward", and "side" corresponding to angular cuts of 90-180°, 9-17°, and 17-90°, respectively. The 90-180° cut corresponded to the back half of the cylinder. The 17-90° cut corresponded to the wall of the cylinder. The 9-17°cut was the foil lining the front face of the cylinder. For each of these angular cuts, there are two samples, Mylar and Al, corresponding to azimuthal angles of 0-180° and 180-360° . Gamma ray spectroscopy of the mylar catcher foil samples and the ^{186}W target was carried out using a well calibrated Ge detector in the ATLAS hot chemistry laboratory. The total observation period was 11 days in which about 15 measurements of each sample were made. The Al catcher foils were dissolved in mineral acid and the Pb isotopes were separated from the solution[57]. Following chemical separation, the Pb isotope fraction was counted on the same Ge detector. The analysis of the γ -ray spectra was done using a modified version of the DECHAOS software [58]. 107 radionuclides were identified in the samples. The end of bombardment (EOB) activities of the nuclides were used to calculate production cross sections taking into account the variable beam intensities using standard equations for the growth and decay of radionuclides during irradiation [59].

III.   RESULTS AND DISCUSSION

The first aspect of the Zagrebaev and Greiner predictions for this reaction that can be checked is the Pb isotopic distribution (Fig. 2). No Pb isotopes were detected in the target, catcher foil or chemical fractions. A rough upper limit cross section for the relevant radionuclides (51.9 h ^{203}Pb and 67.2 m ^{204}Pb^m) is $\sim$ 0.05 mb. Based upon the predictions shown in Figure 2, the expected cross sections for these radionuclides are $\sim$ 3 and 4 mb, respectively. Our observations are thus inconsistent with Figure 2, although it should be noted that the spin and parity of ^{204}Pb^m is 9^- while ^{204}Pb has J$\pi = 0^+$, so that the non-radioactive low spin ground state could still be populated as indicated in Fig. 2 although studies of similar reactions have shown that high spin isomers are preferentially populated[60]. The predicted large cross sections for $^{205-207}$Pb are not observable in this work.

The second aspect of the Zagrebaev and Greiner predictions for this reaction that can be checked are the product angular distributions (Fig. 5). For the three fragment groups (A=130-150, A= 150-190, and A=190-210), we expect their angular distributions to peak

4

at laboratory angles of 80°, 55°, and 35°, respectively or what we term the "side" samples. Our crude three point angular distributions (Fig. 6) for a typical fragment (A=159) agree with this prediction.

The measured nuclidic formation cross sections were placed in seven groups according to mass number (A=43-58, 79-100, 111-140, 146-160, 161-180, 181-190, 191-201). These cross sections were corrected for precursor beta decay, where necessary, by assuming the independent yield cross sections for a given species $\sigma(Z,A)$ can be expressed as a histogram that lies along a Gaussian curve.

$$\sigma(Z, A) = \sigma(A) \left[2\pi C_Z^2(A)\right]^{-1/2} \exp\left[\frac{-(Z - Z_{mp})^2}{2C_Z^2(A)}\right] \tag{1}$$

where $C_Z(A)$ is the Gaussian width parameter for mass number A and $Z_{mp}(A)$ is the most probable atomic number for that A. Using this assumption and the further assumption that $\sigma(A)$ varies slowly and smoothly as a function of A [allowing data from adjacent isobars to be combined in determining $Z_{mp}(A)$ and $C_Z(A)$], one can use the laws of radioactive decay to iteratively correct the measured cumulative formation cross sections for precursor decay.

Within each of the seven groups, the data were fit to a Gaussian-shaped independent yield distribution. The width parameter was found to be constant over a given range in A, while the centers of the charge distributions were adequately represented by linear functions in A over a limited range in A although we expect $Z_{mp}(A)$ to be non-linear. (Only nuclides with well characterized beta-decay precursors and cases where both members of an isomeric pair were observed were included in the analysis). The integration of the independent yield distributions to give the total mass yield corrects for any unobserved radioactive or stable nuclei. The production cross section for ^{187}W (72.7 ± 8.2 mb) was not included in this analysis as it is expected that this nuclide is formed by neutron capture reactions, which are not part of this study. The isobaric yield distribution obtained from this analysis is shown in Figure 7 along with the predictions of Zagrebaev and Greiner. Both the observed and predicted mass distributions are angle integrated. The error bars on the integrated data points reflect the uncertainties due to counting statistics and those introduced in the charge distribution fitting process which have been estimated to be approximately 25 % [61].

At first glance, it appears there are significant differences between the measured and predicted mass distributions. The observed mass yield curve shows two prominent peaks , a broad peak centered at A $\sim$ 140 and a narrow peak centered at A $\sim$ 180. The latter

peak might be associated with the target-like fragments formed in this reaction. A detailed examination of the former group shows there is a narrower prominent peak near A=160 with a plateau of yields extending down to A=120. The product yields from A=70 to A=120 are usually associated with fission fragments from the fission of the target-like nucleus [56]. The fragments with A < 70 are usually taken to be intermediate mass fragments similar to those observed previously in the ^{197}Au + ^{197}Au reaction at energies ≤ 15 MeV/u [62] although the excitation energies in this work are expected to be low given the near barrier projectile energy.

Compared to the known mass distributions for the interaction of 0.5-12 GeV protons with W, the observed distribution is noteworthy because of the lower yields of products from A=160 to A=175. This is presumably due to the lack of spallation processes which operate in high energy proton induced reactions. Some insight into the observed patterns may be gleaned from the predicted [18] excitation energies of the primary fragments, as shown in Figure 8. The low excitation energy (10 MeV) groups are centered near the projectile mass number (between A = 150 and A=170), and near the target mass number of ∼ 186. These groups may be consistent with the broad mass peaks (after de-excitation) centered at A =140 and A=180. The higher excitation energy (40 MeV) group is missing from the observed secondary fragment distribution, perhaps because it has de-excited by fission.

A closer look at the trans-target mass and isotopic yields is shown in Figure 9. In addition to the peak centered at 2-3 amu below the target mass number, enhanced yields are seen for nuclides with A=193 to A=202. While the observed nuclei are not isotopes of Pb (Z_{mp} (196) of the observed nuclides is 79), this broad "goldfinger" is unexpected and is in stark contrast with the usual pattern of steeply decreasing product yields for $A_{product} \geq A_{target}$. A detailed look at the N/Z of these products shows them to be less neutron-rich than the peak yield nuclides as predicted by [18]. Thus one has observed surviving trans-target nuclides in the ^{160}Gd + ^{186}W reaction although they are not in the place predicted by [18]being somewhat closer to the target Z and A. The magnitude of these yields is similar to or greater than those predicted by [18].

IV. CONCLUSIONS

What have we learned in this study? We have

(a) Measured the yields of the reaction products from the 859 MeV ^{160}Gd + ^{186}W reaction using radioanalytical techniques.

(b) Established upper limits for the yields of the Hg and Pb isotopes that are 1-2 orders of magnitude below the predicted yields of [18].

(c) Deduced, from the observed radionuclide yields, a fragment mass distribution for the 859 MeV ^{160}Gd + ^{186}W reaction. That distribution shows yields of intermediate mass fragments, nominal fission fragments and two prominent peaks that are consistent with being the secondary fragment projectile-like and target-like fragments.

(d) Observed enhanced yields of trans-target nuclides in the region of Au that are similar in magnitude (although differing in N and Z) to the shell-stabilized trans-target species predicted by [18].

[1] Y.T. Oganessian, AIP Conference Proceedings **912**, 235 (2007).

[2] S. Hofmann, et al., Z. Phys. A **358**, 377 (1997).

[3] Y.T. Oganessian, J. Phys. G:Nucl. Part. Phys. **34**, R165(2007).

[4] K. Morita, et al., J. Phys. Soc. Japan, **73**, 2593 (2004).

[5] Y.T. Oganessian, et al., Phys. Rev. Lett, **104**, 142502 (2010).

[6] E.M. Kozulin, et al., Phys. Lett. B **686**, 227 (2010).

[7] Y.T. Oganessian, et al., Phys. Rev. C**79** , 024603 (2009).

[8] See G.T. Seaborg and W. Loveland, The Elements Beyond Uranium (Wiley, New York, 1990) for a review of these data.

[9] V.I. Zagrebaev, Y.T. Oganessian, M.G. Itkis and W. Greiner, Phys. Rev. C**73**, 031602(R) (2006).

[10] V. Zagrebaev, and W. Greiner, J. Phys. G **34**, 1 (2007).

[11] V. Zagrebaev, and W. Greiner, J. Phys. G **31**, 825 (2005).

[12] V. Zagrebaev and W. Greiner, J. Phys. G **35**, 125103 (2008).

[13] V. Zagrebaev and W. Greiner, Phys. Rev. Lett **101**, 122701 (2008)

[14] V. Zagrebaev and W. Greiner, CP1098, FUSION08: New Aspects of Heavy Ion Collisions Near the Coulomb Barrier, K.E. Rehm, B.B. Back, H. Esbensen, and C.J. Lister, ed., (AIP, New York, 2009) pp326-333

[15] V. Zagrebaev and W. Greiner, Nucl. Phys. A **834**, 366c (2010).

[16] V. Zagrebaev and W. Greiner, Phys. Rev. C**78**, 034610 (2008).

[17] V. Zagrebaev and W. Greiner,Russ. Chem. Rev. **78**, 1089 (2009).

[18] V. Zagrebaev and W. Greiner, J. Phys. G **34**, 2265 (2007).

[19] Z. Li, X. Wu, and N. Wang, Romanian Rep. in Phys. **59**, 729 (2007)

[20] J.L. Tian, X. Wu, Z. Li and K. Zhao, Chinese Phys. C **32**, 34 (2008).

[21] K. Zhao, X. Wu and z. Li, Phys. Rev. C**80**, 054607 (2009).

[22] W. Loveland, R. J. Otto, D. J. Morrissey and G. T. Seaborg, Phys. Rev. Lett. **39**, 230 (1977).

[23] W. D. Loveland, R. J. Otto, D. J. Morrissey, and G. T. Seaborg, Phys.Lett. **69B**, 284 (1977).

[24] D. J. Morrissey, W. Loveland, R. J. Otto, and G. T. Seaborg, Phys. Lett. **74B**, 35 (1978).

[25] R. J. Otto, D. J. Morrissey, G. T. Seaborg and W. Loveland, Z. Physik A**287**, 97 (1978).

[26] D. J. Morrissey, W. R. Marsh, R. J. Otto, W. Loveland, and G. T. Seaborg, Phys. Rev. C**18**, 1267 (1978).

[27] D. J. Morrissey, W. Loveland, and G. T. Seaborg, Z. Physik A**289**, 123 (1978).

[28] D. J. Morrissey, W. Loveland, M. de SaintSimon and G. T. Seaborg, Phys. Rev. C**21**, 1783 (1980).

[29] W. Loveland, D. J. Morrissey, K. Aleklett, G. T. Seaborg, S. B. Kaufman, E. P. Steinberg, B. D. Wilkins, J. B. Cumming, P. E. Haustein, and H. C. Hseuh, Phys. Rev. C**23**, 253 (1981).

[30] K. Aleklett, D. J. Morrissey, W. Loveland, P. L. McGaughey, and G. T. Seaborg, Phys. Rev. C**23**, 1044 (1981).

[31] W. Loveland, Cheng Luo, P. L. McGaughey, D. J. Morrissey, and G. T. Seaborg, Phys. Rev. C**24**, 464 (1981).

[32] Y. Morita, W. Loveland, P. L. McGaughey, and G. T. Seaborg, Phys. Rev. C**26**, 511 (1982).

[33] B. V. Jacak, W. Loveland, D. J. Morrissey, P. L. McGaughey and G. T. Seaborg, Can. J. Chem. **61**, 701 (1983).

[34] Y. Morita, W. Loveland, and G. T. Seaborg, Phys. Rev. C**28**, 2519 (1983).

[35] R. H. Kraus, Jr., W. Loveland, T. T. Sugihara, K. Aleklett, P. L. McGaughey, G. T. Seaborg, Y. Morita, T. Lund, E. Hagebo, and I.R. Haldorsen, Nucl. Phys. A **432**, 525 (1985).

[36] P. L. McGaughey, W. Loveland, D. J. Morrissey, K. Aleklett, and G. T. Seaborg, Phys. Rev. C**31**, 896 (1985).

[37] 1.W. Loveland, K. Aleklett and G. T. Seaborg. Nucl. Phys. A**447**, 100 (1986).

[38] K. Aleklett, W. Loveland, T. Lund, P. L. McGaughey, Y. Morita, G. T. Seaborg, E. Hagebo, and I.R. Haldorsen, Phys. Rev., C**33**, 885 (1986).

[39] K. Aleklett, W. Loveland, T. T. Sugihara, A. N. Behkami, D. J. Morrissey, Li Wenxin, Wing Kot and G. T. Seaborg. Phys. Scripta **34**, 489 (1986).

[40] W. Loveland, K. Aleklett, L. Sihver, Z. Xu, C. Casey, and G.T. Seaborg, Nucl. Phys. A**471**, 175 (1987).

[41] K. Aleklett, L. Sihver, and W. Loveland, Phys. Lett.B**197**, 34 (1987).

[42] W. Loveland and G.T. Seaborg, Revue de Roumaine de Physique **33**, p. 721737 (1988).

[43] W. Loveland, Z. Xu, C. Casey, K. Aleklett, J.O. Liljenzin, D. Lee and G. T. Seaborg, Phys. Rev. C**38**, 2094 (1988).

[44] C. Casey, W. Loveland, Z. Xu, L. Sihver, K. Aleklett and G. T. Seaborg, Phys. Rev. C**40**,

1244 (1989).

[45] K. Aleklett, W. Loveland, M. de SaintSimon, L. Sihver, J. O. Liljenzin and G. T. Seaborg, Phys. Lett. B**236**, 404 (1990).

[46] W. Loveland, K. Aleklett, L. Sihver, Z. Xu, C. Casey, D. J. Morrissey, J. O. Liljenzin, M. de SaintSimon and G. T. Seaborg, Phys. Rev. C**41**, 973 (1990).

[47] W. Loveland, M. Hellstrom, L. Sihver and K. Aleklett, Phys. Rev. C**42**, 1753 (1990).

[48] L. Sihver, K. Aleklett, W. Loveland, P. L. McGaughey, D. H. E. Gross and H. R. Jaqaman, Nucl. Phys. A**543**, 703 (1992).

[49] A. Yokoyama, W. Loveland, J.O. Liljenzin, K. Aleklett, and D.J. Morrissey, Phys. Rev. C**46**, 647 (1992).

[50] K. Aleklett, R. Yanez, W. Loveland, A. Srivastava, and J.O. Liljenzin, Prog. Part. Nucl. Phys. **30**, 297 (1993).

[51] W. Loveland, K. Aleklett, R. Yanez, A. Srivastava, and J.O. Liljenzin, Phys. Lett. B**276**, 311 (1993).

[52] R. Yanez, W. Loveland, K. Aleklett, A. Srivastava, and J.O. Liljenzin, Phys. Rev. C**52**, 203 (1995).

[53] R. Yanez, W. Loveland, D.J. Morrissey, K. Aleklett, J.O. Liljenzin, E. Hagebo, D. Jerrestam and L.Westerberg, Phys. Lett. B**376**, 29 (1996).

[54] W. Loveland,M. Andersson, K.E. Zyromski, N. Ham, B. Altschul, J. Vlcakova, D. Menge, J.O. Liljenzin, R. Yanez, and K. Aleklett, Phys Rev. C**59**, 1472 (1999).

[55] R.W. Stoenner, R.L. Klobuchar, P.E. Haustein, G.J. Virtes, J.B. Cumming, and W. Loveland, Phys. Rev. C **73**, 047602 (2006).

[56] Y. Asano, et al., J. Phys. Soc. Japan, **54**, 3734 (1985); ibid, **57**, 2995 (1988).

[57] NAS-NS-3040, The radiochemistry of lead, W.M. Gibson, USAEC. 1961, Procedure 11

[58] K. Aleklett, J. O. Liljenzin, and W. Loveland, J. Radioanal. Nucl. Chem. **193**, 187 (1996).

[59] G. Friedlander, J.W. Kennedy, E. S. Macias, and J. M. Miller, Nuclear and Radiochemistry, 3rd Edition (Wiley, New York, 1981) p191.

[60] J.V. Kratz, W. Brüchle, G. Franz, M. Schädel, I. Warneke, G. Wirth and M. Weis, Nucl. Phys. A **332**, 447 (1979).

[61] D.J. Morrissey, W. Loveland, M. de Saint-Simon, and G.T. Seaborg, Phys. Rev. C **21**, 1783 (1980).

[62] Th. Blaich, J.V. Kratz, R. Schmoll, K. Sümmerer, and G. Wirth, Z. Phys. A **356**, 49 (1996).

[63] T.C. Awes, R.L. Ferguson, R. Novotny, F.E. Obenshain, F. Plasil, S. Pontoppidan, V. Rauch, G.R. Young, and H. Sann, Phys. Rev. Lett **52**, 251 (1984).

[64] O.B. Tarasov and D. Bazin, Phys. At. Nuclei **66**, 1578 (2003).
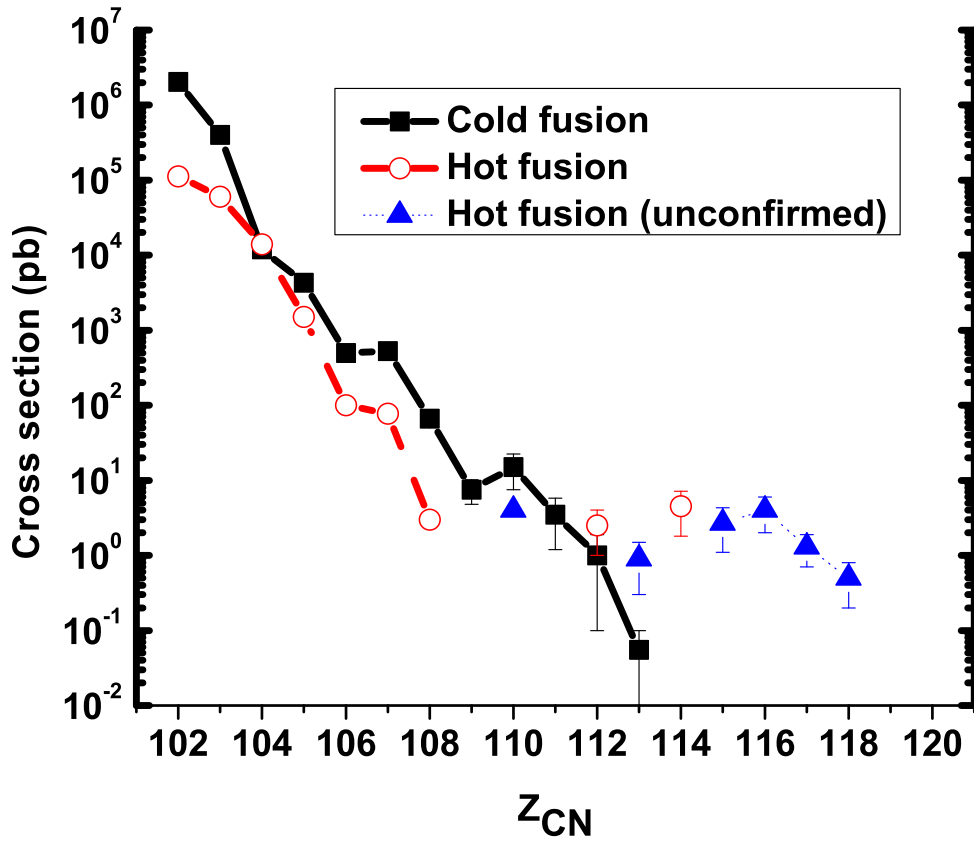
FIG. 1: (Color online)Measured cross sections for the production of the heaviest elements. Experimental data are from [1–5]"Unconfirmed" means the observation has not been repeated by another laboratory
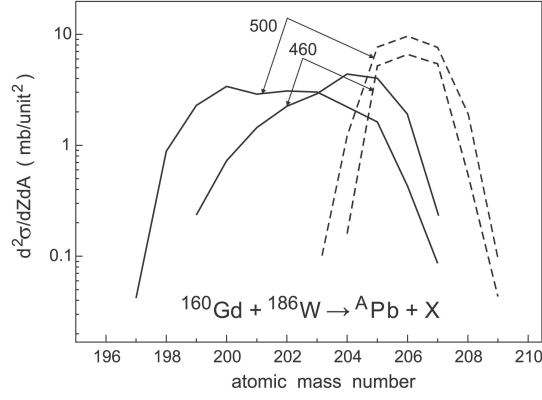
FIG. 2: Predicted [18] Pb isotopic distribution for the ^{160}Gd + ^{186}W. reaction. The labels 500 and 460 refer to the c.m. energies of the ^{160}Gd. The solid lines are the final product distributions after particle evaporation while the dashed lines refer to the primary product distributions. (Reproduced from Ref. [13] with permission.)
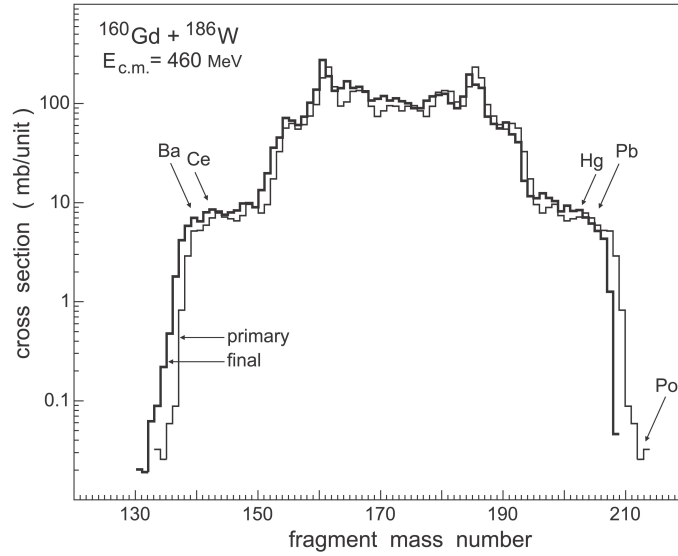
FIG. 3: Predicted [18] mass distribution for the products of the ^{160}Gd + ^{186}W reaction. The terms "primary" and "final" refer to the product distributiions before and after particle evaporation. (Reproduced from Ref. [13] with permission.)
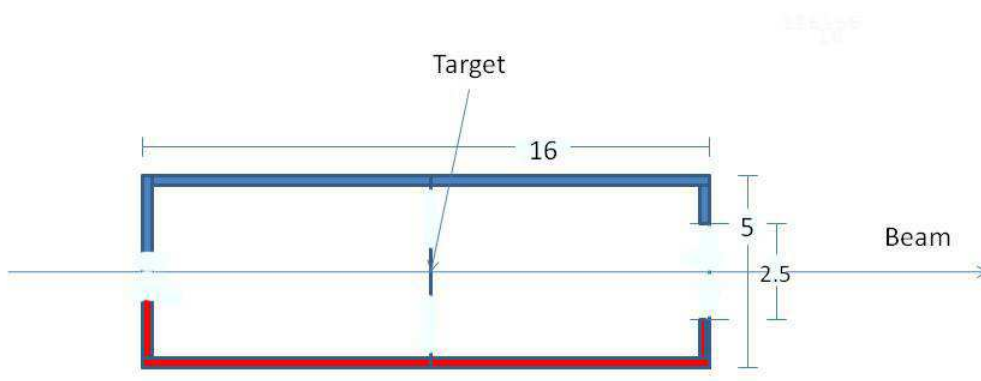
FIG. 4: (Color online) Schematic diagram of the experimental apparatus. All dimensions are given in cm. (For more details see text.)
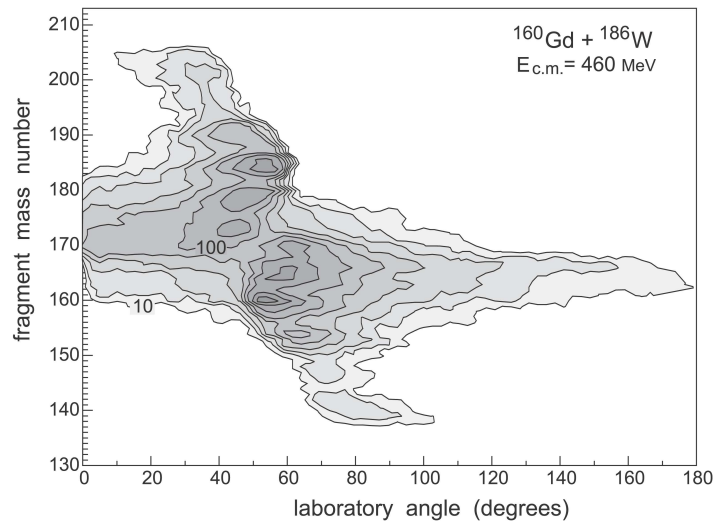

FIG. 5: Predicted [18] angular distribution of the reaction products from the ^{160}Gd + ^{186}W reaction. (Reproduced from Ref. [13] with permission.)
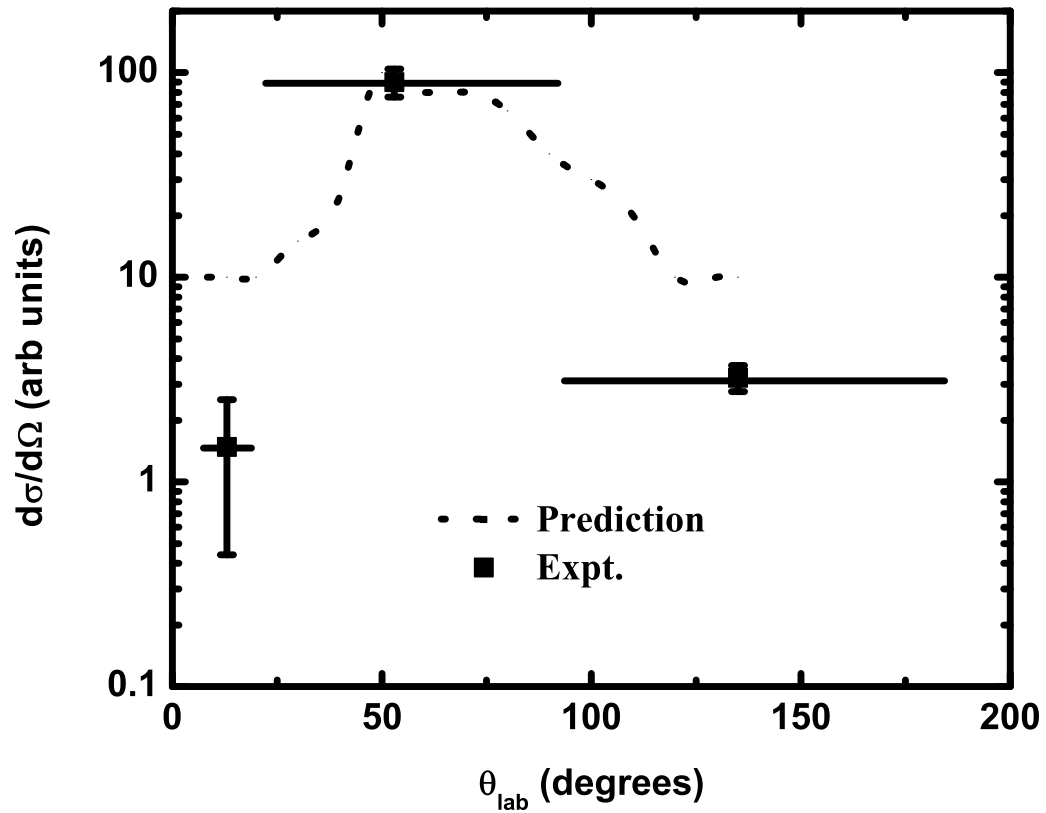
FIG. 6: Comparison of predicted [18] and observed angular distributions for a typical reaction product with A = 159. For the observed angular distributions, the horizontal lines indicate the angular range of the "detector" while the vertical error bars indicate the statistical uncertainty in the result.
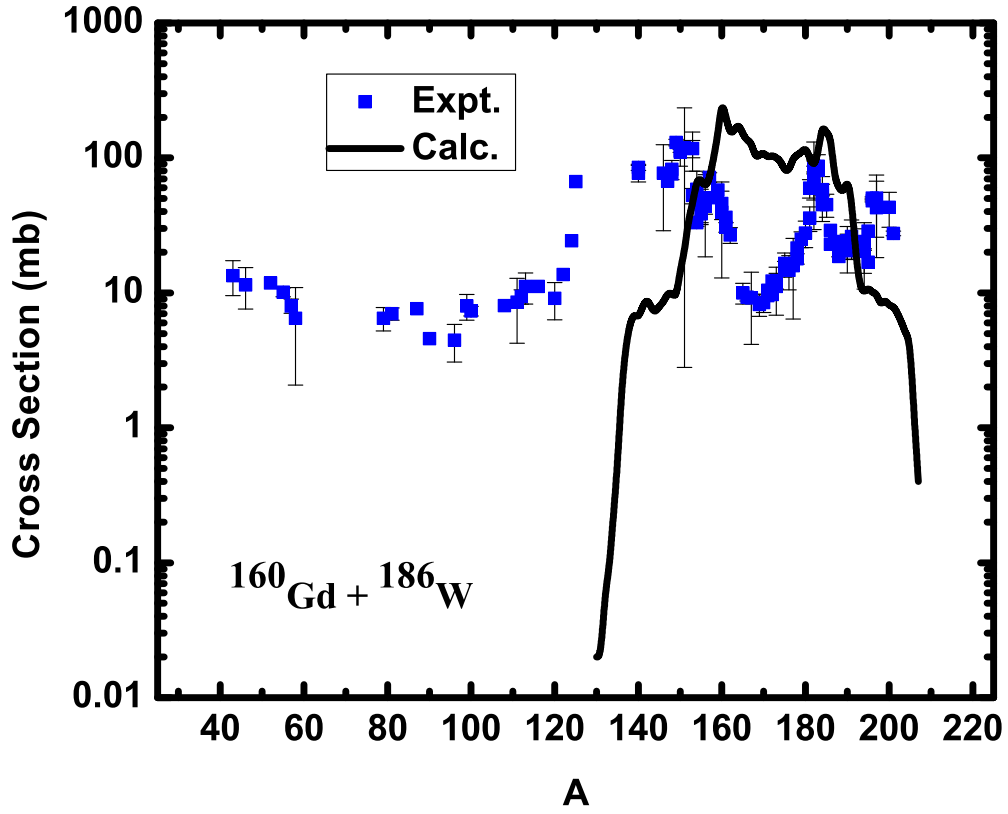
FIG. 7: (Color online)Predicted [18] and observed mass distributions for the ^{160}Gd + ^{186}W reaction.
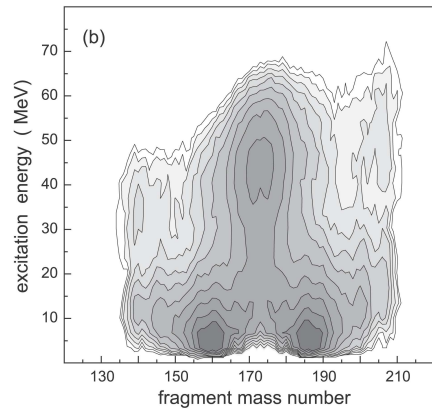
FIG. 8: Predicted [18] primary fragment excitation energies for the ^{160}Gd + ^{186}W reaction. (Reproduced from Ref. [13] with permission.)
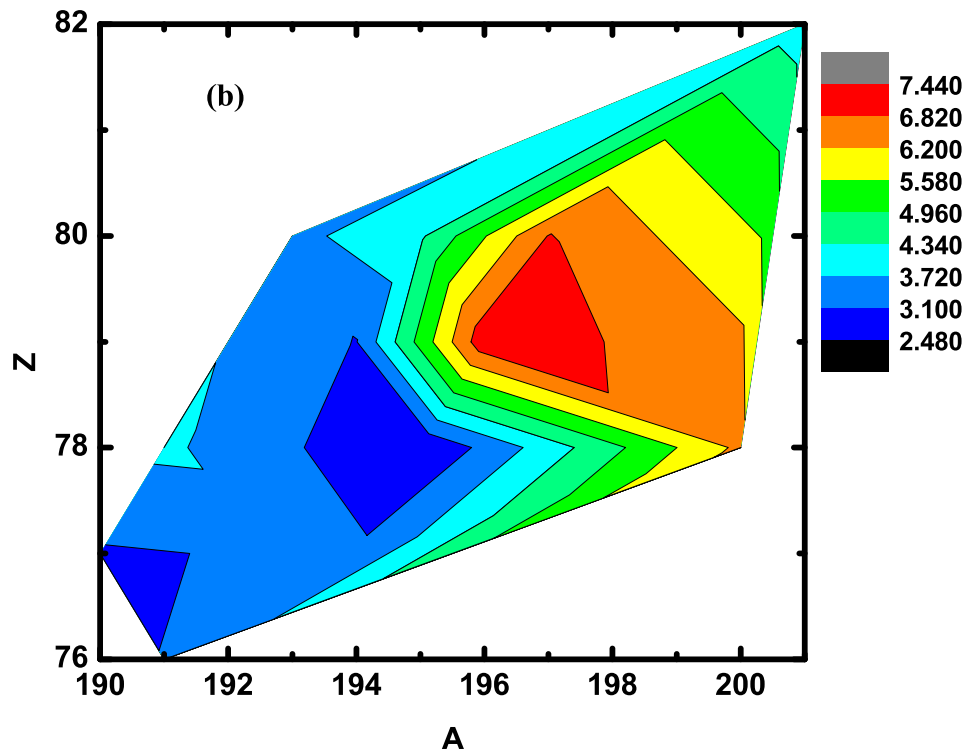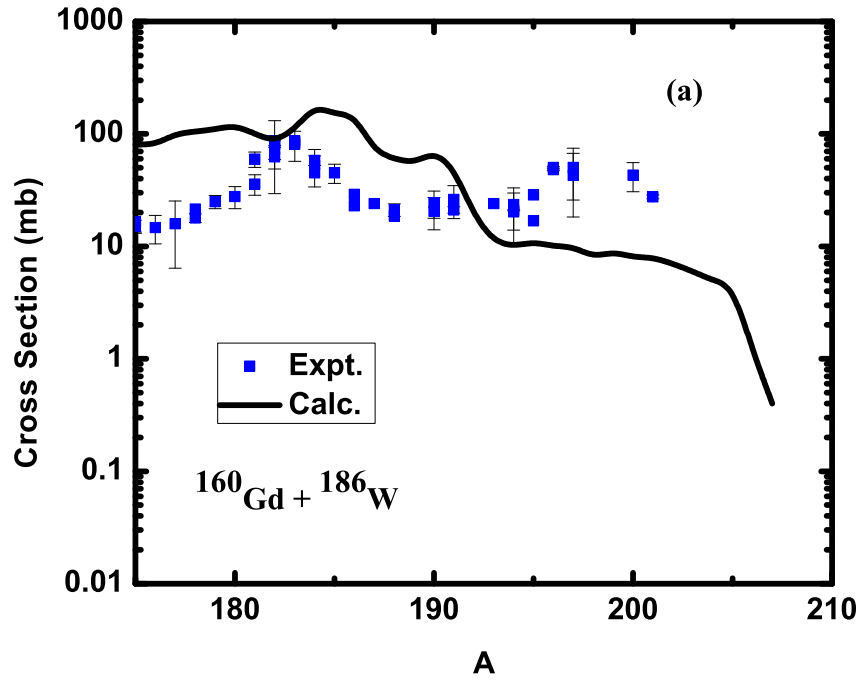
FIG. 9: (a) Predicted [18] and observed mass distributions for trans-target nuclides from the ^{160}Gd + ^{186}W reaction. (b) (Color online) Contour plot of observed nuclidic yields in the trans-target region